Chemical Science

ROYAL SOCIETY OF CHEMISTRY

EDGE ARTICLE

View Article Online
View Journal | View Issue

Cite this: *Chem. Sci.*, 2024, **15**, 16210

All publication charges for this article have been paid for by the Royal Society of Chemistry

Received 9th June 2024
Accepted 8th September 2024

DOI: 10.1039/d4sc03781b

rsc.li/chemical-science

Metal-free alkyne annulation enabling π-extension of boron-doped polycyclic aromatic hydrocarbons†

Mandala Anitha,[a] To-Jen Chin,[a] Guan-Cheng Liu,[a] Chi-Tien Hsieh,[b] Kuan-Hua Wang,[b] Shu-Li Li,[a] Mu-Jeng Cheng [b] [b] and Jeffrey M. Farrell *[ac]

A C–H functionalizing annulation reaction of boron-doped polycyclic aromatic hydrocarbons (PAHs) with alkynes is described. This metal-free π-extension provides a new synthetic route to fusion atom B-doped polycyclic aromatic hydrocarbons (PAHs) that is demonstrated with the synthesis of a family of new, functionalized, structurally constrained 6a,15a-diborabenzo[*tuv*]naphtho[2,1-*b*]picenes. These annulation products exhibit deep LUMO energy levels, strong visible-range absorptions, and sterically accessible π-systems that can adopt herringbone or π-stacked solid-state structures based on choice of substituents. From regioselectivity and DFT calculations, we propose an annulation mechanism involving intramolecular electrophilic aromatic substitution of a zwitterionic intermediate.

Introduction

Molecular polycyclic aromatic hydrocarbon (PAH) substructures of graphene exhibit remarkable opto(electronic) properties and supramolecular behaviors that have led to their pivotal roles in modern functional organic materials.[1] The replacement of PAH carbon atoms with one or more heteroatoms, or "heteroatom-doping," has become an indispensable tool to modify optical and electronic properties while retaining PAH geometries.[2] Substitution of PAH carbon atoms with neutral, three-coordinate boron renders them electron-deficient. Accordingly, B-doped PAHs are positioned to satisfy growing demands for electron-poor π-systems in applications including n-type semiconductor materials.[3] Encouragingly, B-doped PAHs have been demonstrated in organic transistors,[4] as non-fullerene acceptors in organic solar cells,[5] as thermally activated delayed fluorescence emitters in organic light-emitting diodes,[6] and for small molecule activations.[7]

Synthetic challenges remain for B-doped PAHs. For example, "structurally constrained"[8] B-doped PAHs with boron substitutions at fusion positions (shared by two or more of the fused rings) are rare, despite attractive characteristics (Fig. 1).[9] These fusion B-doped PAHs are kinetically stabilized by structural constraint, so sterically bulky substituents are not needed to protect boron from nucleophilic attack.[8] Consequently, ambient stability can be achieved while retaining unobstructed π-surfaces that could form π-stacked structures suited for charge-carrier transport. In addition, few existing syntheses produce B-doped PAHs bearing desirable "deep" LUMO energy levels, defined by Ingleson, Zysman-Colman, and co-workers as less than −3.0 eV.[10] This property is highly dependent on π-core shape, size, and boron substitution pattern.[5,11] Moreover, common co-dopants (*e.g.* N) can contribute electron pairs to the π-conjugated system, offsetting LUMO-lowering contributions of boron's empty p orbital.[12] Finally, functionalized periphery substituents are often difficult to install due to chemical sensitivities typical of organoboranes and their syntheses.

Strategies towards fusion B-doped PAHs include oxidative cyclodehydrogenation[9a,11,13] or Ni-mediated ring–closing reactions[9b,9d] of properly substituted aryl boranes. Additionally, electrophilic borylation[9c] (sometimes followed by rearrangement)[9e] has proven useful in recent syntheses.[9f,9h] Nevertheless, the field lacks the extensive synthetic tools available for

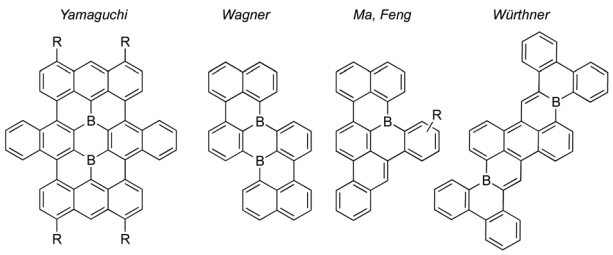

Fig. 1 Examples of structurally constrained polybenzenoid fusion atom B-doped PAHs.[9a,9d–f]

[a]*Department of Chemistry, National Taiwan University, No. 1, Sec. 4, Roosevelt Rd., Taipei 10617, Taiwan. E-mail: farrell@ntu.edu.tw*

[b]*Department of Chemistry, National Cheng Kung University, Tainan 701, Taiwan*

[c]*Center for Emerging Materials and Advanced Devices, National Taiwan University, No. 1, Sec. 4, Roosevelt Rd., Taipei 10617, Taiwan*

† Electronic supplementary information (ESI) available. CCDC 2341631 2341632 2341633 2341634 2341635 2341636. For ESI and crystallographic data in CIF or other electronic format see DOI: https://doi.org/10.1039/d4sc03781b

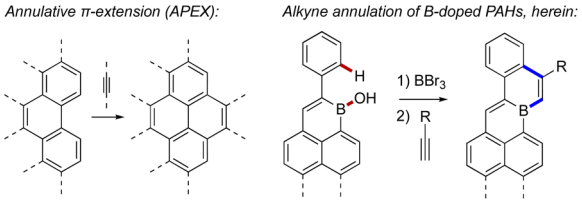

Fig. 2 A schematic example of annulative π-extension[14] (left) compared to the alkyne annulation of B-doped PAHs described herein (right).

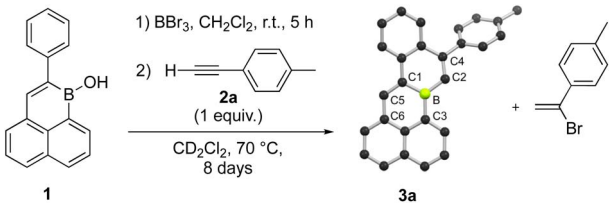

Scheme 1 Formation of **3a** by bromination of **1** followed by alkyne annulation. Compound **3a** is illustrated by its solid-state structure. C: black, B: yellow-green, H atoms omitted for clarity.

other classes of PAHs. Elsewhere, intermolecular annulative π-extension (or "APEX")[14] has become a valuable strategy for π-scaffold construction (Fig. 2), where the modular annulation of π-fragments allows elaboration of many products from a single polyaromatic precursor. Analogous π-extensions of B-doped π-scaffolds could alleviate the shortage of fusion B-doped PAHs, as annulations with different partners would sharply increase available structures. This could also allow B-doped PAHs bearing unprecedented shapes, sizes, substitution patterns, and functional groups to be realized, opening new avenues for the discovery and use of B-doped π-conjugated structures.

Herein we report an unanticipated metal-free, regioselective annulation reaction of a boron-doped PAH with a terminal alkyne. DFT calculations suggest this reactivity proceeds *via* intramolecular electrophilic aromatic substitution of a zwitterionic intermediate. The reaction was applied to the synthesis of a family of functionalized, fusion atom B-doped PAHs. Annulated products exhibited red-shifted absorption and emission spectra as well as substantially more positive reduction potentials compared to their precursors. DFT calculations corroborated low LUMO energy levels of the annulated products, and implied antiaromatic character of their boron-containing six-membered rings. Fusion B-doped PAHs synthesized herein are amongst the lowest-LUMO B-doped PAHs yet reported and exhibit solid-state packing arrangements that can be tailored by choice of alkyne annulation partner.

Results and discussion

We began our study by probing the reactivity of polycyclic borinic acid 1-hydroxy-2-phenyl-1-boraphenalene, **1**.[5] Excess BBr_3 was reacted with **1** in CH_2Cl_2 at room temperature for five hours to effect –OH for –Br exchange. After removal of volatiles *in vacuo*, the residue was dissolved in CD_2Cl_2 and reacted with *p*-tolylacetylene at 70 °C in a sealed J Young NMR tube (Scheme 1). As the reactants were gradually consumed over 8 days, the formation of two major products could be observed by ^{1}H NMR spectroscopy (Fig. S1 and S2†). One product was identified as the Markovnikov addition product of HBr to *p*-tolylacetylene, 1-(1-bromoethenyl)-4-methylbenzene. To our surprise, the other major reaction product could be identified as **3a**, an annulation product with a bond formed between B and the alkyne terminal C, as well as a new C–C bond from an apparent C–H functionalization of the boraphenalene phenyl substituent (Scheme 1). Compound **3a** crystalized from CD_2Cl_2 solution and its planarized structure could be confirmed by single-crystal X-ray crystallography. Further ^{1}H NMR spectroscopy studies were conducted to optimize this reactivity (Table S1†). Rate of **3a** formation could be increased by undertaking the reaction at 120 °C in C_6D_5Br. Noting that the overall transformation requires two equivalents of alkyne per annulation, 2 : 1 stoichiometry of alkyne : borane also improved conversion to **3a**. Under these improved conditions, **3a** could be isolated in 33% yield after recrystallization from 1 : 1 CH_2Cl_2 : hexane. When BCl_3 was employed in the –OH for halogen exchange step, the annulation was comparatively sluggish. As well, no formation of **3a** was observed in the direct reaction between borinic acid **1** and *p*-tolylacetylene under the same conditions. We speculate that Lewis acid strength of the boron center is critical to the reaction. At 120 °C in C_6D_5Br for 180 h, diphenylacetylene and 1-phenyl-1-propyne each fail to react with **1** (after –OH for –Br exchange), indicating possible steric limitations of annulation reactivity. In attempts to sequester generated HBr with exogenous bases, reactions were undertaken using one equivalent each of alkyne and base (2,6-di-*tert*-butyl-4-methylpyridine, 2,6-dichloropyridine, 2,6-lutidine, or 2,2,6,6-tetramethylpiperidine) under otherwise optimized conditions (Table S1†). While inhibited formation of 1-(1-bromoethenyl)-4-methylbenzene was observed by ^{1}H NMR spectroscopy for the latter two stronger bases, none of the basic additives improved conversions to **3a**.

This annulation is markedly different to the reactions of alkynes with 5-membered boracyclic 9-halo-9-borofluorenes, for which alkyne insertion *via* 1,2-carboboration has been shown by Fukushima and co-workers.[15] Other possible outcomes, such as 1,1-carboboration[16] or haloboration,[17] are apparently not favored under the given reaction conditions. The regioselectivity of the annulation of **1** after –OH for –Br exchange might suggest the involvement of a vinyl cation generated by attack of the boron center by the alkyne triple bond. Prerequisite resonance stabilization of such an intermediate[18] (enroute to electrophilic aromatic substitution) would explain the observed positioning of the tolyl group in the major annulation product. Moreover, related intermediates, generated by the combination of alkynes and boranes, are implicated in the $B(C_6F_5)_3$-mediated cascade syntheses of dibenzopentalenes of Yamaguchi, Erker, and co-workers,[19] and in boron trihalide-mediated borylative cyclizations of Ingleson and co-workers.[20] Indeed, Ingleson and co-workers have utilized the latter strategy to construct edge B-doped PAHs using combinations of well-designed alkynes and

boron trihalides.[21] However, unlike these examples which react alkynes with strong external Lewis acids, the present reaction between a brominated edge-B-doped PAH and an external alkyne must presumably rely on a much weaker Lewis acidic center for generation of a vinyl cation intermediate. The feasibility of this mechanistic proposal was not obvious to us, so we examined it using DFT calculations at the B3LYP-D3(BJ)/def2-TZVP//B3LYP-D3(BJ)/def2-SVP level (see ESI† for details). Indeed, an enthalpic local minimum was found for a vinyl cation-containing intermediate, generated from attack on boron by the alkyne triple bond (Fig. 3, **3a-2**). The charge assignment on **3a-2** is supported by our Natural Population Analysis calculation; specifically, from reactants to **3a-2**, the charge on the vinyl cation (C highlighted in red) increased by 0.38 e^-, while the charge on boron decreased by 0.19 e^-. The calculated pathway to form **3a** *via* the ring closing from intermediate **3a-2** involves an intramolecular electrophilic aromatic substitution reaction, and its highest enthalpic barrier (7.0 kcal mol^{-1}) is calculated for the C–C bond forming step of the annulation (Fig. 3, **3a-2** → **3a-3**). In contrast, the enthalpy profile of the formation of an alternative regioisomer of **3a** (wherein the positions of the alkyne substituents are reversed) possessed a higher enthalpic barrier (23.6 kcal mol^{-1}) for product formation, and no enthalpic local minimum for a vinyl cation-containing intermediate (Fig. S71†).

We sought to apply this unusual intermolecular annulation to the synthesis of extended B-doped PAHs. As a target, we identified 6a,15a-diborabenzo[*tuv*]naphtho[2,1-*b*]picene as a B-doped core structure for which a potential precursor borinic acid, **4**, has already been reported.[5] Furthermore, DFT calculations suggest that 6a,15a-diborabenzo[*tuv*]naphtho[2,1-*b*]picenes should possess desirable low-LUMO energy levels and visible range absorptions (Table S4 and Fig. S62†). Thus, we conducted a series of experiments where **4** was reacted with BBr_3 in CH_2Cl_2 at room temperature for 22 h and, after removal of volatiles *in vacuo*, further reacted with four equivalents of alkyne in C_6H_5Cl at 120 °C for 60 h. The resulting B-doped PAHs **5a–j** were isolated in 3–24% yield as ambient-stable purple-to-black solids after solvent washing steps, filtration through celite in $CHCl_3$ solution, and solvent removal *in vacuo* (Scheme 2). Aryl-, alkyl-, and alkenyl-substituted alkynes of varying electron-demand could be successfully employed in annulation reactions. Notably, thiophene, alkene, and ester functional groups are tolerated. No annulation products could be isolated from reactions with *p*-(trifluoromethyl)phenylacetylene or *p*-methoxyphenylacetylene, the former of which we speculate may be complicated by B-mediated fluoride abstraction.[22] Assigned structures of poorly soluble **5a–j** were confirmed using ^{1}H NMR spectroscopy at elevated temperatures, solid-state ^{13}C NMR spectroscopy, and high-resolution mass spectrometry. Solid samples of 6a,15a-diborabenzo[*tuv*]naphtho[2,1-*b*]picenes stored in ambient conditions for one week showed no indication of decomposition by ^{1}H NMR spectroscopy.

Crystals of **5a**, **5c**, **5d**, **5f**, and **5g** suitable for X-ray crystallography could be obtained *via* sublimation (<10^{-6} torr, 390–420 °C). Solid-state structures confirmed anticipated polyaromatic structures with planar cove-free π-cores. Planarities about B centers are indicated by sums of C–B–C bond angles of 360° for each (*e.g.* Fig. 4a). The periphery C–B–C bond angles (*e.g.* Fig. 4a, C2–B–C3) are slightly enlarged from an ideal 120°, measuring 125°–126°. The B–C bonds of **5a**, **5c**, **5d**, **5f**, and **5g** are 1.52–1.56 Å, slightly shorter than typical-B–C(sp^2) single bonds (*e.g.* BPh_3 B–C = 1.57–1.59 Å),[23] but in line with B–C single bonds in other fusion atom B-doped systems.[9a,9f] In addition, C2–C4 and C1–C5 double bonds are slightly elongated

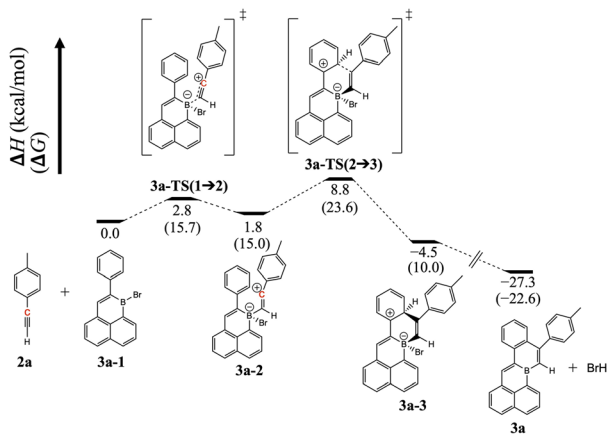

Fig. 3 DFT-calculated enthalpy and Gibbs free energy profile of the formation of **3a**. The structures were optimized in CPCM solvation model in CH_2Cl_2.

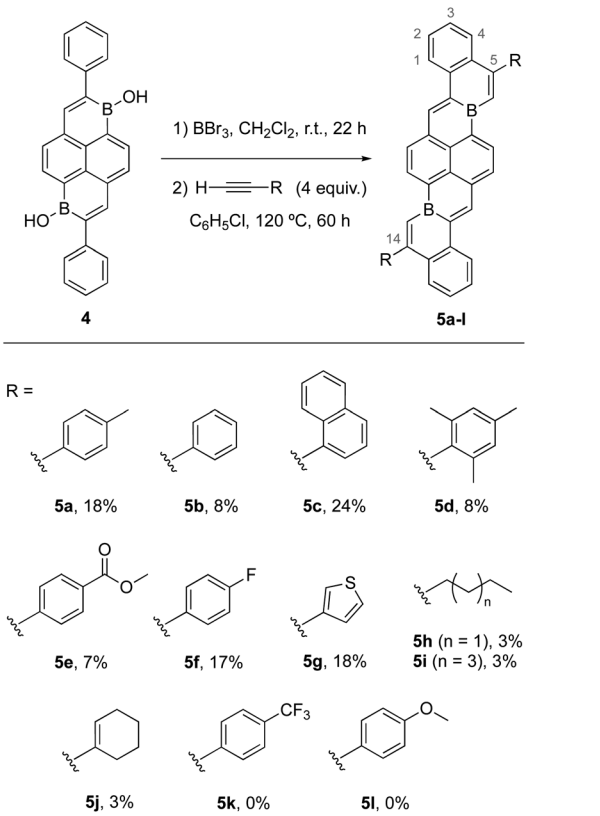

Scheme 2 Annulative syntheses of extended fusion atom B-doped PAHs.

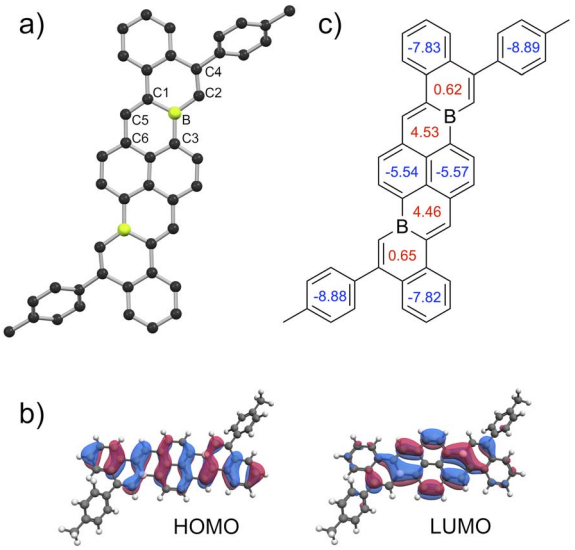

Fig. 4 (a) Solid-state structure of **5a** determined by X-ray crystallography. C: black, B: yellow-green, H atoms omitted for clarity. (b) Frontier molecular orbitals of **5a** from DFT calculations (isosurfaces = 0.07 Å^{-3}). (c) NICS(1) values calculated for rings of **5a** (B3LYP-D3(BJ)/def2-TZVP//B3LYP-D3(BJ)/def2-SVP).

compared to typical C–C double bonds, while C5–C6 bonds are slightly short for single bonds. Analogous bonding trends are observed for **3a** (Scheme 1). These data suggest effective delocalization over B-doped π-surfaces, consistent with our DFT calculations that indicate highly delocalized frontier molecular orbitals (Fig. 4b, Table S4†). The delocalization of the LUMOs in combination with the structurally constrained environments of boron might temper the Lewis acidities of boron centers, contributing to the ambient stabilities of **5a–j**. To understand the aromaticity of these π-systems, representative NICS[24] analyses of **3a** and **5a** were performed (Fig. 4c and S74†). NICS(0) and NICS(1) calculations indicate that six-membered rings containing boron and a vinylic double bond are significantly less aromatic than carbon-only six-membered rings. These data are consistent with previous aromaticity assessments reported for B-doped PAHs.[9f,9h]

Solid-state packing structures of **5a**, **5c**, **5d**, **5f**, and **5g** were dramatically influenced by substituent variations in the 5 and 14 position (Fig. 5a). The π-cores of mesityl-substituted **5d** arrange into a herringbone structure with several close intermolecular C–H···π distances (2.6–3.1 Å) between B-doped π-cores. Conversely, π-cores of 3-thienyl-substituted **5g** form continuous columnar π-stacks with significant overlap between π-systems and ∼3.4 Å interplanar distances (Fig. 5b). Interestingly, these stacks are composed of distinct trimeric sub-stacks of molecules of **5g** in two different thienyl orientations, wherein the roll angle between molecules within each trimer is slightly reduced compared to the roll angle between trimers (Fig. 5c and S70).[25] We note that C–H···π interactions between thienyl substituents of **5g** are indicated by close proximities of ∼2.8 Å (Fig. 5c, dotted lines). The packings of **5c**, **5f**, and **5a** show a continuum between the herringbone packing of **5d** and the π-stacked packing of **5g** (Fig. 5a).

UV-Vis spectra of **5a–j** in *o*-$C_6H_4Cl_2$ (10^{-6}–10^{-5} M, 298 K) show strong visible absorptions with lowest energy λ_{abs} between 546–563 nm and ε ranging 1.9–3.6 × 10^4 L mol^{-1} cm^{-1}. For **3a** the lowest energy λ_{abs} is 445 nm with ε = 8.3 × 10^3 L mol^{-1} cm^{-1} (Fig. 6a and Table 1). These lowest energy absorption maxima are all considerably red-shifted compared to respective precursors **4** (λ_{abs} = 425 nm) and **1** (λ_{abs} = 374 nm) in $CHCl_3$,[5] reflecting the extended conjugation of the annulated products and correlating well with TD-DFT predicted spectra (Fig. S72 and S73†). Fluorescence emission maxima of annulated compounds in *o*-$C_6H_4Cl_2$ (10^{-6}–10^{-5} M, 298 K) are also red-shifted compared to those of precursors **4** (λ_{em} = 561 nm) and **1** (λ_{em} = 489 nm) in $CHCl_3$.[5] Compounds **5a–j** show emissions with λ_{em} ranging 601–616 nm and low quantum yields ($\Phi \leq$ 0.03, Table S2 and Fig. S63†). These emissions correspond to apparent Stokes shifts between 1220–1760 cm^{-1}. Compound **3a**

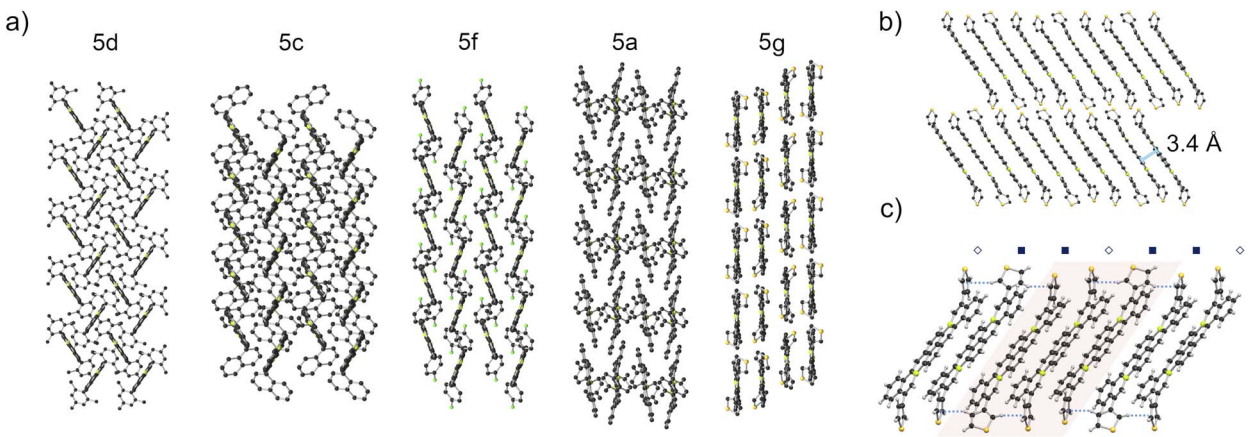

Fig. 5 (a) Side-on views of solid-state packing structures of **5d**, **5c**, **5f**, **5a**, and **5g**. (b) Alternate view of the π-stacked structure of **5g**. (c) Diagram illustrating close contacts of thienyl groups of **5g** and highlighting a representative trimeric sub-stack (red) of **5g** molecules with two different 3-thienyl orientations (labelled with diamonds or squares). C: black, B: yellow-green, F: green S: yellow, H: grey, selected H atoms omitted for clarity.

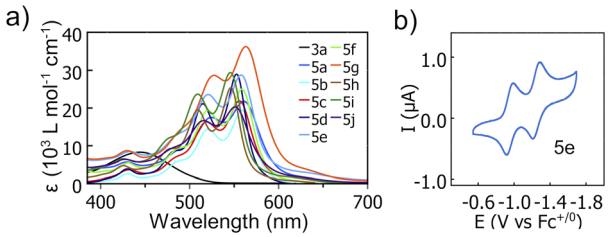

Fig. 6 (a) UV-Vis spectra of **3a** and **5a–j** (10^{-6}–10^{-5} M in *o*-$C_6H_4Cl_2$, 298 K). (b) Cyclic voltammogram of **5e** (9.0×10^{-4} M in 0.1 M *n*-Bu_4NPF_6 *o*-$C_6H_4Cl_2$, 298 K).

Table 1 Summary of optical and electronic properties of **3a** and **5a–j**.[a]

	λ_{abs} [nm], (ε [M^{-1} cm^{-1}])	λ_{em} [nm]	$E_{1/2\ red\ 1}$ [V]	$E_{1/2\ red\ 2}$ [V]
3a	365 (4500), 445 (8300)	587	−1.62	—
5a	429 (5700), 525 (17 500), 561 (21 800)	608	−1.01	−1.33
5b	431 (2600), 521 (14 400), 559 (19 400)	603	−0.98	−1.29
5c	432 (3600), 519 (16 300), 556 (21 900)	607	−0.97	−1.29
5d	430 (3900), 515 (21 100), 553 (29 000)	610	−1.00	−1.49
5e	433 (8500), 521 (23 600), 558 (28 800)	607	−0.95	−1.24
5f	431 (5500), 520 (19 400), 559 (25 000)	616	−0.97	−1.26
5g	430 (8700), 527 (28 700), 563 (36 200)	616	−0.99	−1.30
5h	425 (4700), 510 (19 400), 546 (25 400)	604	−1.05	−1.36
5i	426 (6500), 509 (23 700), 546 (29 400)	601	−1.08	−1.39
5j	427 (6400), 516 (16 600), 551 (20 300)	607	−1.02	−1.33

[a] Optical measurements were performed at 10^{-6}–10^{-5} M concentrations in *o*-$C_6H_4Cl_2$ at 298 K. Cyclic voltammetry experiments were performed at 10^{-4}–10^{-3} M concentrations in 0.1 M *n*-Bu_4NPF_6 *o*-$C_6H_4Cl_2$ at 298 K and referenced *vs.* $Fc^{+/0}$ using ferrocene as an internal standard. All other experimental details are described in the ESI.

(8.5×10^{-6} M in *o*-$C_6H_4Cl_2$, 298 K) exhibits broad emission (λ_{em}, = 587 nm) and a quantum yield of 0.14.

Cyclic voltammetry was used to probe the electrochemical properties of **3a** and **5a–j**, (10^{-4}–10^{-3} M in 0.1 M *n*-Bu_4NPF_6 *o*-$C_6H_4Cl_2$, 298 K, Table 1). A single reversible one-electron reduction was observed for **3a**, and two reversible one-electron reductions were observed for each compound **5a–j** (*e.g.* Fig. 6b and S52–S61†). The compounds studied exhibited +0.36–+0.52 V more positive first reduction potentials ($E_{1/2\ red\ 1}$) than their non-annulated precursors **1** and **4** (reported in CH_2Cl_2).[5] Strikingly, first reduction potentials of **5a-j** (−0.95–−1.08 V *vs.* $Fc^{+/0}$) are amongst the most positive yet reported for boron-doped PAHs, and are all more positive (by +0.09–+0.22 V) than $E_{1/2\ red\ 1}$ reported for $PC_{61}BM$ in the same solvent.[26] These $E_{1/2\ red\ 1}$ values correspond to very low estimated LUMO energy levels of −4.20–−4.07 eV.[27] We note that **5a**, **5c**, **5d**, **5f**, and **5g** each bear "deep LUMO"[10] energy levels and exhibit similar strong visible range absorptions. However, they adopt solid-state packing motifs ranging from herringbone to continuous π-stacks. This embodies "heteroatom-doping" as a means to modify optical and electronic properties largely independently of molecular geometries and substituents, allowing the latter to be used for the control of solid-state packing.

Conclusions

We report a C–H-functionalizing annulation reaction of B-doped PAHs with alkynes. This reactivity complements existing B-doped PAH syntheses with a facile π-extension methodology for the synthesis of structurally constrained, fusion atom B-doped PAHs. We applied this synthetic strategy to ambient-stable, deep LUMO energy 6a,15a-diborabenzo[*tuv*]naphtho[2,1-*b*]picenes, whose solid-state packing can be directed *via* substituent effects. Annulation leads to red-shifted absorption and emission spectra, as well as significantly more positive reduction potentials, compared to corresponding B-doped PAH precursors. We anticipate that this new synthetic tool will aid the development and use of B-doped π-conjugated structures. Studies to this end are underway in our laboratory.

Data availability

All experimental details and data supporting this article are available in the ESI.†

Author contributions

A. M. and T.-J. C. performed the synthetic experiments. G.-C. L. measured optical and electronic properties. S.-L. L. performed solid-state NMR measurements. C.-T. H. and K.-H. W. performed DFT calculations. M.-J. C. directed DFT studies. J. M. F. supervised the research and wrote the manuscript. All authors edited the manuscript.

Conflicts of interest

There are no conflicts to declare.

Acknowledgements

We are grateful for the financial support of the National Science and Technology Council of Taiwan (grant no. 110-2113-M-002-028-MY3) and the Yushan Young Scholar Program of the Ministry of Education of Taiwan. We acknowledge the mass spectrometry technical research services from Consortia of Key Technologies, National Taiwan University and the Instrumentation Center of National Taiwan Normal University. We also thank Mr Yi-Hung Liu (NTU) for X-ray crystal structure determination. We thank Prof. Pi-Tai Chou (NTU), Prof. Ken-Tsung Wong (NTU) for use of their laboratory's spectrometers and CVD equipment. We are also grateful to Prof. Jerry C. C. Chan (NTU) for assistance with solid-state NMR measurements.

Notes and references

1 A. Narita, X.-Y. Wang, X. Feng and K. Müllen, *Chem. Soc. Rev.*, 2015, **44**, 6616.
2 (*a*) M. Stępień, E. Gońka, M. Żyła and N. Sprutta, *Chem. Rev.*, 2017, **117**, 3479; (*b*) X.-Y. Wang, X. Yao, A. Narita and K. Müllen, *Acc. Chem. Res.*, 2019, **52**, 2491; (*c*) A. Borissov,

Y. K. Maurya, L. Moshniaha, W.-S. Wong, M. Żyła-Karwowska and M. Stępień, *Chem. Rev.*, 2022, **122**, 565.

3 (*a*) S. Yamaguchi and A. Wakamiya, *Pure Appl. Chem.*, 2006, **78**, 1413; (*b*) E. von Grotthuss, A. John, T. Kaese and M. Wagner, *Asian J. Org. Chem.*, 2018, **7**, 37; (*c*) S. K. Mellerup and S. Wang, *Trends Chem.*, 2019, **1**, 77.

4 (*a*) K. Matsuo, S. Saito and S. Yamaguchi, *Angew. Chem., Int. Ed.*, 2016, **55**, 11984; (*b*) T. Kushida, S. Shirai, N. Ando, T. Okamoto, H. Ishii, H. Matsui, M. Yamagishi, T. Uemura, J. Tsurumi, S. Watanabe, J. Takeya and S. Yamaguchi, *J. Am. Chem. Soc.*, 2017, **139**, 14336.

5 J. M. Farrell, C. Mützel, D. Bialas, M. Rudolf, K. Menekse, A.-M. Krause, M. Stolte and F. Würthner, *J. Am. Chem. Soc.*, 2019, **141**, 9096.

6 (*a*) T.-L. Wu, M.-J. Huang, C.-C. Lin, P.-Y. Huang, T.-Y. Chou, R.-W. Chen-Cheng, H.-W. Lin, R.-S. Liu and C.-H. Cheng, *Nat. Photonics*, 2018, **12**, 235; (*b*) C.-M. Hsieh, T.-L. Wu, J. Jayakumar, Y.-C. Wang, C.-L. Ko, W.-Y. Hung, T.-C. Lin, H.-H. Wu, K.-H. Lin, C.-H. Lin, S. Hsieh and C.-H. Cheng, *ACS Appl. Mater. Interfaces*, 2020, **12**, 23199.

7 (*a*) E. von Grotthuss, M. Diefenbach, M. Bolte, H. W. Lerner, M. C. Holthausen and M. Wagner, *Angew. Chem., Int. Ed.*, 2016, **55**, 14067; (*b*) E. von Grotthuss, S. E. Prey, M. Bolte, H.-W. Lerner and M. Wagner, *Angew. Chem., Int. Ed.*, 2018, **57**, 16491; (*c*) J. E. Barker, A. D. Obi, D. A. Dickie and R. J. Gilliard Jr, *J. Am. Chem. Soc.*, 2023, **145**, 2028.

8 (*a*) Z. Zhou, A. Wakamiya, T. Kushida and S. Yamaguchi, *J. Am. Chem. Soc.*, 2012, **134**, 4529; (*b*) M. Hirai, N. Tanaka, M. Sakai and S. Yamaguchi, *Chem. Rev.*, 2019, **119**, 8291.

9 (*a*) C. Dou, S. Saito, K. Matsuo, I. Hisaki and S. Yamaguchi, *Angew. Chem., Int. Ed.*, 2012, **51**, 12206; (*b*) K. Schickedanz, T. Trageser, M. Bolte, H.-W. Lerner and M. Wagner, *Chem. Commun.*, 2015, **51**, 15808; (*c*) F. Miyamoto, S. Nakatsuka, K. Yamada, K.-i. Nakayama and T. Hatakeyama, *Org. Lett.*, 2015, **17**, 6158; (*d*) J. Radtke, K. Schickedanz, M. Bamberg, L. Menduti, D. Schollmeyer, M. Bolte, H.-W. Lerner and M. Wagner, *Chem. Sci.*, 2019, **10**, 9017; (*e*) J.-J. Zhang, L. Yang, F. Liu, Y. Fu, J. Liu, A. A. Popov, J. Ma and X. Feng, *Angew. Chem., Int. Ed.*, 2021, **60**, 25695; (*f*) C. Mützel, J. M. Farrell, K. Shoyama and F. Würthner, *Angew. Chem., Int. Ed.*, 2022, **61**, e202115746; (*g*) W. Sun, J. Guo, Z. Fan, L. Yuan, K. Ye, C. Dou and Y. Wang, *Angew. Chem., Int. Ed.*, 2022, **61**, e202209271; (*h*) J. Guo, K. Zhang, Y. Wang, H. Wei, W. Xiao, K. Yang and Z. Zeng, *Chem. Sci.*, 2023, **14**, 4158.

10 K. Yuan, A. K. Gupta, C. Si, M. Uzelac, E. Zysman-Colman and M. J. Ingleson, *Org. Lett.*, 2023, **25**, 5880.

11 Y. Liu, L. Yuan, J. Guo, W. Sun, Y. Wang and C. Dou, *Angew. Chem., Int. Ed.*, 2023, **62**, e202306911.

12 Nevertheless, heteroatom/B co-doped nanographenes have impressive applications, see: M. Mamada, M. Hayakawa, J. Ochi and T. Hatakeyama, *Chem. Soc. Rev.*, 2024, **53**, 1624.

13 H. Narita, H. Choi, M. Ito, N. Ando, S. Ogi and S. Yamaguchi, *Chem. Sci.*, 2022, **13**, 1484.

14 (*a*) E. H. Fort, P. M. Donovan and L. T. Scott, *J. Am. Chem. Soc.*, 2009, **131**, 16006; (*b*) H. Ito, K. Ozaki and K. Itami, *Angew. Chem., Int. Ed.*, 2017, **56**, 11144.

15 Y. Shoji, N. Tanaka, S. Muranaka, N. Shigeno, H. Sugiyama, K. Takenouchi, F. Hajjaj and T. Fukushima, *Nat. Commun.*, 2016, **7**, 12704.

16 G. Kehr and G. Erker, *Chem. Commun.*, 2012, **48**, 1839.

17 M. F. Lappert and B. Prokai, *J. Organomet. Chem.*, 1964, **1**, 384.

18 M. B. Goldfinger and T. M. Swager, *J. Am. Chem. Soc.*, 1994, **116**, 7895.

19 C. Chen, M. Harhausen, R. Liedtke, K. Bussmann, A. Fukazawa, S. Yamaguchi, J. L. Petersen, C. G. Daniliuc, R. Fröhlich, G. Kehr and G. Erker, *Angew. Chem., Int. Ed.*, 2013, **52**, 5992.

20 A. J. Warner, J. R. Lawson, V. Fasano and M. J. Ingleson, *Angew. Chem., Int. Ed.*, 2015, **54**, 11245.

21 (*a*) D. L. Crossley, R. J. Kahan, S. Endres, A. J. Warner, R. A. Smith, J. Cid, J. J. Dunsford, J. E. Jones, I. Vitorica-Yrezabal and M. J. Ingleson, *Chem. Sci.*, 2017, **8**, 7969; (*b*) R. J. Kahan, D. L. Crossley, J. Cid, J. E. Radcliffe and M. J. Ingleson, *Angew. Chem., Int. Ed.*, 2018, **57**, 8084; (*c*) K. Yuan, R. J. Kahan, C. Si, A. Williams, S. Kirschner, M. Uzelac, E. Zysman-Colman and M. J. Ingleson, *Chem. Sci.*, 2020, **11**, 3258.

22 T. Stahl, H. F. T. Klare and M. Oestreich, *ACS Catal.*, 2013, **3**, 1578.

23 F. Zettler, H. D. Hausen and H. Hess, *J. Organomet. Chem.*, 1974, **72**, 157.

24 Z. Chen, C. S. Wannere, C. Corminboeuf, R. Puchta and P. v. R. Schleyer, *Chem. Rev.*, 2005, **105**, 3842.

25 M. D. Curtis, J. Cao and J. W. Kampf, *J. Am. Chem. Soc.*, 2004, **126**, 4318.

26 J. C. Hummelen, B. W. Knight, F. LePeq, F. Wudl, J. Yao and C. L. Wilkins, *J. Org. Chem.*, 1995, **60**, 532.

27 LUMO energy levels estimated using the equation: $E_{LUMO} = -e(E^{1/2}\ \text{red}) - 5.15$ eV. Adapted from: C. M. Cardona, W. Li, A. E. Kaifer, D. Stockdale and G. C. Bazan, *Adv. Mater.*, 2011, **23**, 2367.